Proceedings of the 2018 IEEE/ASME International Conference on Advanced Intelligent Mechatronics (AIM), Auckland, New Zealand, July 9-12, 2018

A calculation method for the stability lobes of 3-DOF Boring *

Zhihang Lin, Pingfa Feng, Jianfu Zhang*, *Member, IEEE*, Dingwen Yu, Zhijun Wu

***Abstract*—Large length–diameter ratios in boring bars of weak rigidity cause chatter vibration of the cutting system during the boring process. Stability lobes are widely used for analyzing and describing the stability of cutting systems. To decrease the possibility of chatter and improve efficiency and surface quality in boring deep holes, a method of calculating the stability lobes for boring with three degrees of freedom (3-DOF) is proposed, which considers both regenerative chatter and modal-coupling chatter. Based on the classical cutting force model and 3-DOF equations of motion, the relationship between the dynamic cutting forces and displacements was deduced using a cutting force model and the geometric relationship between cutting thickness and displacement. The stability lobes of a boring bar with holes were analyzed and the results verified the effectiveness of the proposed calculation method.**

I. Introduction

With increasing demand for high-precision deep-hole parts, such as hydraulic gas cylinders, weapon launchers, and precision instruments, there are higher demands for machining efficiency and the quality of surfaces processed using precision and ultra-precision deep-hole machining technology. Precision boring is an important technology in deep-hole machining. Under certain extreme manufacturing conditions, the length–diameter ratio of the boring bar leads to poor rigidity of the cutting system and the processing is prone to generate chatter, which damages the quality of the processing surface and reduces processing efficiency. To reduce chatter during the boring of a weak rigid system, it is necessary to study the mechanical behavior of the boring process and consider the influence of the time-varying load. The widely recognized chatter mechanisms include regenerative chatter, modal-coupling chatter, hysteresis effects, and frictional effects. Of these, regenerative chatter and modal-coupling chatter are the main mechanisms [1].

The many studies of chatter can be divided into two main categories: the establishment of chatter models and the development of calculation algorithms for the stability lobes. Many models for chatter caused by different mechanisms have been established. Tlusty [2] and Sisson [3] studied causes of friction-type chatter; Gasparetto studied the vibration–stabilization conditions of modal-coupling-type chatter [4]; Iturrospe presented a state space method to analyze modal-coupling-type chatter [5]; Tlusty developed a set of linear regenerative chatter theories [6]. Various algorithms have been proposed to calculate the stability lobes more efficiently and accurately: Altintas proposed the zero order solution [7, 8]; Merdol proposed the multi-frequency method [9]. Based on the semi-discretization method proposed by Insperger [10], Ding proposed the full-discretization method based on numerical integration [11]. Other methods include the temporal finite-element method proposed by Bayly [12], time-domain simulations method proposed by Tlusty [13], and the cutting force peak–peak time-domain simulation model established by Smith [14]. In addition to these investigations concerning theoretical calculation algorithms for the stability lobes, experimental measurements that support verification of the algorithms have also been studied [15, 16]. These studies were, however, mainly aimed at milling processes, with few studies on the stability of boring. Moreover, most studies only considered two degrees of freedom (2-DOF) in machining stability; there is little literature concerning boring stability under three degrees of freedom (3-DOF), which represents the actual situation more closely.

In this work, boring forces were modeled in three directions and the relationship between the force and displacement in the directions of three degrees of freedom was obtained by force and geometric analyses. Based on the second-order full-discretization method, a method for calculating the stability lobes of 3-DOF boring chatter was proposed. Finally, stability lobes of boring bars with holes of different diameters were calculated at different angles using this method. The results were consistent with the experimental results, which proved the effectiveness and practicability of the proposed approach.

II. Modeling and Analysis

A. Boring force model

The structure of a deep-hole boring machine is very different from that of a milling machine, as shown in Fig. 1. Its structural characteristics are that the boring bar and workpiece have large aspect ratios. During processing of a deep hole, the boring tools used are one-insert boring heads. In actual processing, it is found that chatter is more likely to occur when the cutting thickness is increased, which greatly reduces the processing efficiency and the quality of the machined surface.

*Research supported by the National Nature Science Foundation of China (Grant No. 51575301), and Shenzhen Foundational Research Project (Grant No. JCYJ20160428181916222).

Pingfa Feng and Jianfu Zhang* are with the State Key Laboratory of Tribology and Beijing Key Lab of Precision/Ultra-precision Manufacturing Equipments and Control, Tsinghua University, Beijing 100084, China (*corresponding author to provide e-mail: zhjf@tsinghua.edu.cn).

Pingfa Feng is with the Graduate School at ShenZhen, Tsinghua University, ShenZhen 518055, China

All authors are with the Department of Mechanical Engineering, Tsinghua University, Beijing 100084, China.

978-1-5386-1854-7/18/$31.00 ©2018 IEEE

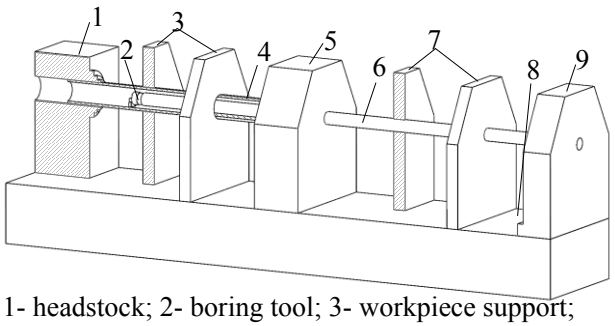

1- headstock; 2- boring tool; 3- workpiece support; 4 - workpiece; 5 - oiler; 6 - boring bar;7 - boring bar support frame; 8 - bed; 9 - boring bar drive;

Figure 1. Structure of deep-hole boring machine.

The main differences between a boring and milling process are that, for boring:

- The teeth of the boring tool are in contact with the workpiece all the time during the machining;
- During the boring process, the relative angle and position formed by the boring tool and the machined surface do not change with time.

A boring force model must be established to study the stability of the boring process. The total boring force can be decomposed into components in three directions: the tangential force F_t, the radial force F_r, and the feed force F_f. In general, the cutting forces models are [1]:

$$F_t=K_t b_D h_D; \quad (1)$$

$$F_r=K_r b_D h_D; \quad (2)$$

$$F_f=K_f b_D h_D, \quad (3)$$

where K_t, K_r, K_f are the cutting force coefficients, b_D is the cutting width, and h_D is the cutting thickness. Cutting parameters of a boring process are shown in Fig. 2, where a_p is the depth of cutting, f is the feed, and κ_r is the tool cutting edge angle.

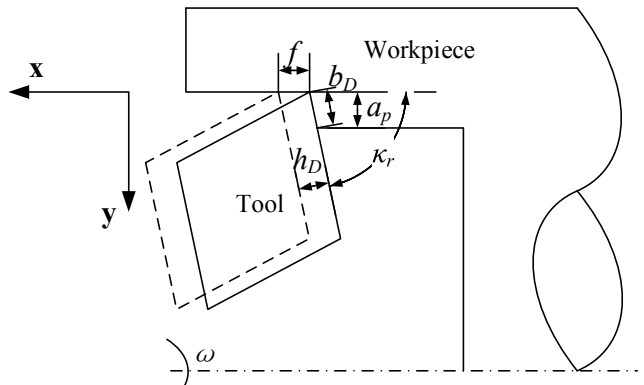

Figure 2. Cutting parameters of a boring process.

B. Dynamic model of 3-DOF boring

Actual boring chatter is extremely complex, so the following assumptions were made to facilitate modeling and calculation:

- According to research [1], regenerative chatter and modal-coupling chatter are the main chatter mechanisms in tool cutting, so the effects of other mechanisms were ignored;
- The workpiece is a weak rigid structure with a large aspect ratio in real processing, which will affect the chatter: to simplify modeling, this work only considered the influence of the tool;
- In actual machining, the reference system of tool angles will change due to the feed movement, non-equal height between the tip and center of the workpiece, non-vertical or non-parallel center line installation of the tool bar, and other factors, which means that working angles and static angles are unequal: this paper ignored the effects of these factors;
- There are many modes of the tool system: to simplify modeling, only a single mode of the tool in the three main directions was considered.

The 3-DOF boring model is shown in Fig. 3, where x_1, x_2, x_3 are the three main mode directions of the boring bar; k_1, k_2, k_3 are the modal stiffnesses and c_1, c_2 , c_3 are the modal dampings in the x_1, x_2, x_3 directions, respectively; ω is the rotational angular velocity of the workpiece; F_0 is the static component of the cutting force; ΔF is the dynamic component of the cutting force; y is the normal direction of the workpiece surface; x is feed direction. F' and y' are the projections of F_0 and y on the x_1–x_2 planes, respectively. The angle between y and x_1 is θ, and the angle between y and F_0 is θ_0.

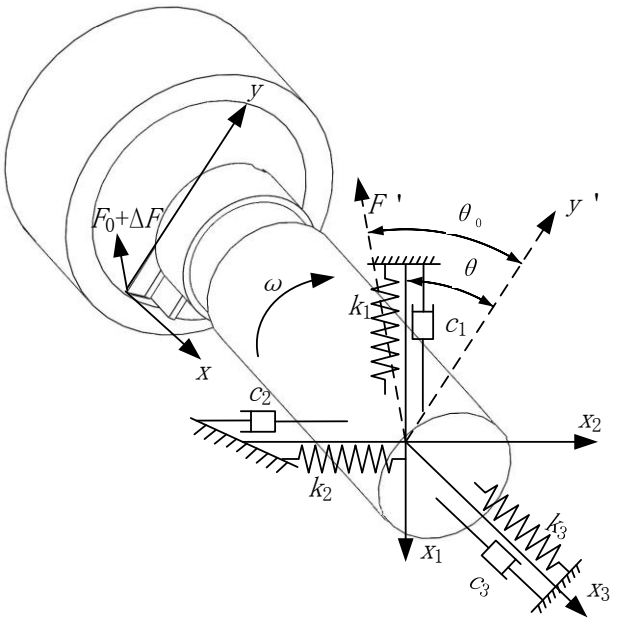

Figure 3. 3-DOF boring model.

The 3-DOF equation of motion is given by:

$$\begin{bmatrix} m_1 & & \\ & m_2 & \\ & & m_3 \end{bmatrix} \begin{bmatrix} \ddot{x}_1 \\ \ddot{x}_2 \\ \ddot{x}_3 \end{bmatrix} + \begin{bmatrix} c_1 & & \\ & c_2 & \\ & & c_3 \end{bmatrix} \begin{bmatrix} \dot{x}_1 \\ \dot{x}_2 \\ \dot{x}_3 \end{bmatrix} + \begin{bmatrix} k_1 & & \\ & k_2 & \\ & & k_3 \end{bmatrix} \begin{bmatrix} x_1 \\ x_2 \\ x_3 \end{bmatrix} = \begin{bmatrix} -\Delta F_1 \\ -\Delta F_2 \\ -\Delta F_3 \end{bmatrix}, \quad (4)$$

where m_1, m_2, m_3 are the effective masses of the boring bar in the x_1, x_2, x_3 directions, respectively.

According to the geometric relationship in Fig. 2, h_D could be expressed as:

$$\Delta h_D = \begin{bmatrix} \cos(\kappa_r) \\ \sin(\kappa_r) \end{bmatrix}^T \begin{bmatrix} \Delta y \\ \Delta x \end{bmatrix}, \tag{5}$$

where Δx is Δx_3. According to the geometric relationship in Fig. 3, Δy could be expressed as:

$$\Delta y = \begin{bmatrix} \cos(\theta) \\ \sin(\theta) \end{bmatrix}^T \begin{bmatrix} \Delta x_1 \\ \Delta x_2 \end{bmatrix}, \tag{6}$$

So the cutting thickness model is given by:

$$\Delta h_D = \begin{bmatrix} \cos(\theta)\cdot\cos(\kappa_r) \\ \sin(\theta)\cdot\cos(\kappa_r) \\ \sin(\kappa_r) \end{bmatrix}^T \begin{bmatrix} \Delta x_1 \\ \Delta x_2 \\ \Delta x_3 \end{bmatrix}, \tag{7}$$

According to Equations (1)–(3) for the simplified boring force model, the following relationship could be obtained:

$$\Delta F_f = K_f b_D \Delta h_D; \tag{8}$$

$$\Delta F_{rt} = \sqrt{K_r^2 + K_t^2}\, b_D \Delta h_D, \tag{9}$$

where ΔF_{rt} is the resultant force of ΔF_r and ΔF_t. ΔF_{rt} and ΔF_f are decomposed along the axes of Fig. 3 and F is decomposed along the directions of x_1, x_2. The following relationships could hence be obtained:

$$\begin{bmatrix} \Delta F_1 \\ \Delta F_2 \\ \Delta F_3 \end{bmatrix} = \begin{bmatrix} -\cos(\kappa_r)\cos(\theta_0-\theta) & -\sin(\kappa_r)\cos(\theta_0-\theta) & 0 \\ -\cos(\kappa_r)\sin(\theta_0-\theta) & -\sin(\kappa_r)\sin(\theta_0-\theta) & 0 \\ -\sin(\kappa_r) & \cos(\kappa_r) & 0 \end{bmatrix} \begin{bmatrix} \Delta F_f \\ \Delta F_{rt} \\ 0 \end{bmatrix}, \tag{10}$$

Substituting (8) and (9) into (10), the relationships between dynamic forces and dynamic displacements in the directions of 3-DOF could be obtained:

$$\begin{bmatrix} \Delta F_1 \\ \Delta F_2 \\ \Delta F_3 \end{bmatrix} = b_D \begin{bmatrix} -\cos(\kappa_r)\cos(\theta_0-\theta) & -\sin(\kappa_r)\cos(\theta_0-\theta) & 0 \\ -\cos(\kappa_r)\sin(\theta_0-\theta) & -\sin(\kappa_r)\sin(\theta_0-\theta) & 0 \\ -\sin(\kappa_r) & \cos(\kappa_r) & 0 \end{bmatrix} \begin{bmatrix} K_f \\ \sqrt{K_r^2 + K_t^2} \\ 0 \end{bmatrix} \begin{bmatrix} \cos(\theta)\cdot\cos(\kappa_r) \\ \sin(\theta)\cdot\cos(\kappa_r) \\ \sin(\kappa_r) \end{bmatrix}^T \begin{bmatrix} \Delta x_1 \\ \Delta x_2 \\ \Delta x_3 \end{bmatrix} \tag{11}$$

Because θ was included, regenerative chatter and modal-coupling chatter could be represented by the model.

III. Calculation of Stability Lobes of 3-DOF Boring

The procedures of the second-order full-discretization method for 3-DOF boring were deduced as follows: (4) was reduced to an equation of tool motion that contains both excitation parameter and time-delay terms:

$$M\ddot{q}(t) + C\dot{q}(t) + Kq(t) = b_D K_c(t)\left[q(t) - q(t-T)\right] + f_0(t), \tag{12}$$

where M, C, and K are the modal mass, the damping, and the stiffness matrix of the tool, respectively; $q(t)$ is the coordinate of tool modes, $q(t) = [x_1, x_2, x_3]^T$; and T is the delay and equal to the cutting period of the cutter tooth, where $T = 60/\omega$. For a linear force model, the static force $f_0(t)$ does not affect the stability, so $f_0(t)$ can be omitted, and (12) degenerates into:

$$M\ddot{q}(t) + C\dot{q}(t) + Kq(t) = b_D K_c(t)\left[q(t) - q(t-T)\right], \tag{13}$$

Defining $p(t)=Mq'(t)+Cq(t)/2$ and $x(t) = [q(t), p(t)]^T$, Equation (13) can be transformed into the following state space form:

$$\dot{x}(t) = Ax(t) + B(t)x(t) - B(t)x(t-T) \tag{14}$$

where A is a constant matrix representing the invariant property of the system, $B(t)$ is the periodic matrix determined by the dynamic cutting force considering the regenerative effect and $B(t+T) = B(t)$, and T is the time period and equal to the delay. The equations are given by:

$$A = \begin{bmatrix} -M^{-1}C/2 & M^{-1} \\ \dfrac{CM^{-1}C}{4} - K & CM^{-1}/2 \end{bmatrix} \tag{15}$$

$$B_{3\times3}(t) = b_D \begin{bmatrix} \cos(\kappa_r)\cos(\theta_0-\theta) & \sin(\kappa_r)\cos(\theta_0-\theta) & 0 \\ \cos(\kappa_r)\sin(\theta_0-\theta) & \sin(\kappa_r)\sin(\theta_0-\theta) & 0 \\ \sin(\kappa_r) & -\cos(\kappa_r) & 0 \end{bmatrix} \begin{bmatrix} K_f \\ \sqrt{K_r^2 + K_t^2} \\ 0 \end{bmatrix} \begin{bmatrix} \cos(\theta)\cdot\cos(\kappa_r) \\ \sin(\theta)\cdot\cos(\kappa_r) \\ \sin(\kappa_r) \end{bmatrix}^T \tag{16}$$

$$B(t) = -\begin{bmatrix} 0 & 0 \\ B_{3\times3}(t) & 0 \end{bmatrix} \tag{17}$$

where $B(t)$ is a 6×6 matrix. Taking A, $B_{3\times3}(t)$, $B(t)$ into the second-order full-discretization method [17], the stability lobes of a 3-DOF boring machine could be calculated. The flow chart of the algorithm is shown in Fig. 4.

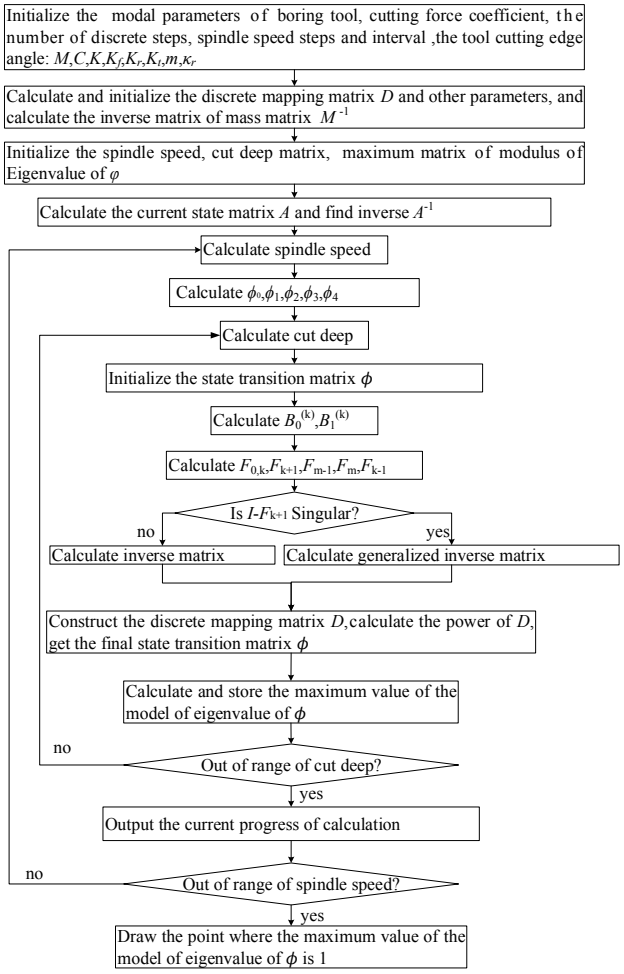

Figure 4. Flow chart showing algorithm to solve stability lobes of 3-DOF boring.

IV. Calculating Stability Lobe Diagrams

Using the theoretical derivation above and the flow chart shown in Fig. 4, the corresponding code was obtained in Matlab R2015a. Boring bars with holes referred from [18], shown as Fig. 5, were analyzed using the proposed calculation method. The detailed conditions of the experiments are shown: boring bars with holes were installed in an ordinary lathe CA6140 to cut workpieces and two CD-1 speed sensors(Heng Odd Instrument Co. Ltd, Beijing, China) were placed in the horizontal and vertical directions to measure the displacements of vibration of the boring bars in these directions. The materials of the workpieces and boring tool were 45# steel and high-speed steel, respectively. The specific dimensions and cutting force coefficients are shown in Table I. The cross terms in the matrix M,K,C of (4) were ignored.

TABLE I. SPECIFIC PARAMETERS OF BORING SYSTEM

d(mm)	ξ	θ(°)	θ_0(°)	K_f,K_r,K_t(N/m^2)	κ_r(°)
0,8,10,12,15,18,20,25	0.005	0,30,60,90,120,150	33	2×10^9, 6×10^9,4×10^9	30

After obtaining the size parameters given in Table I, the effective mass and corresponding frequencies in the x_1, x_2, x_3 directions for boring bars with different sized parameters were calculated using finite-element analysis. These results are shown in Fig. 6, using d = 25 mm as an example; the detailed results are listed in Table II.

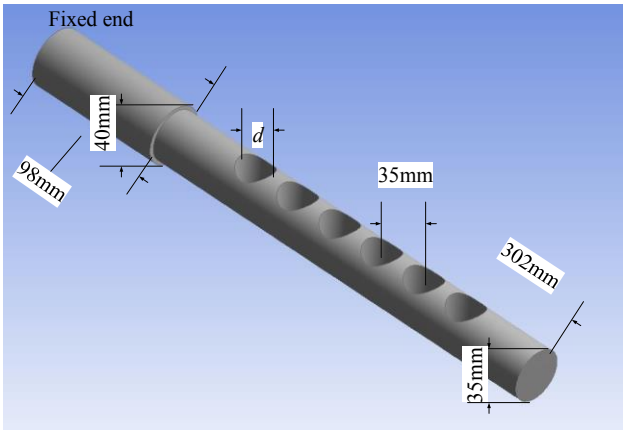

Figure 5. Parameters of boring bar analyzed.

TABLE II. FREQUENCY AND EFFECTIVE MASS PARAMETERS OF BORING SYSTEM AS CALCULATED BY FINITE-ELEMENT SIMULATION

direction / d(mm)	frequency(rad/s)			effective mass (kg)		
	x_1	x_2	x_3	x_1	x_2	x_3
0	1140.7	1140.5	20932.2	1.14	1.14	2.45
8	1135.0	1157.6	20731.3	1.69	1.71	2.32
10	1128.8	1166.8	20565.6	1.64	1.68	2.25
12	1119.4	1177.7	20345.1	1.57	1.63	2.16
15	1095.6	1196.2	19875.9	1.45	1.54	1.99
18	1054.1	1215.3	19218.9	1.30	1.43	1.80
20	1011.8	1226.5	18641.8	1.19	1.34	1.65
25	830.4	1229.2	16441.5	0.89	1.09	1.24

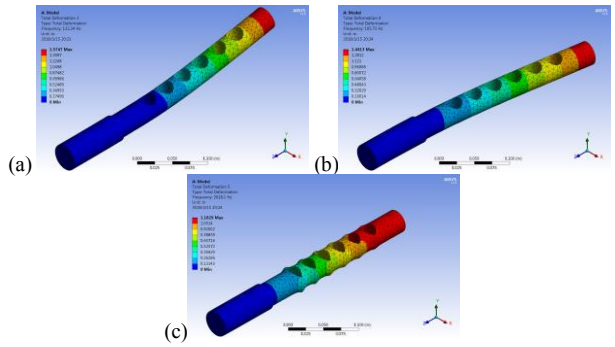

Figure 6. Finite-element analysis results in (a) x_1, (b) x_2, and (c) x_3 directions.

The stability lobes of boring systems with holes of different diameters are shown in Fig. 7. The impacts of various parameters on the stability of boring were obtained from Fig. 8 and the improvement of holes on chatter of the boring bar was obtained by comparing Fig. 8 with Fig. 9. The chatter status at the test point X (a_p = 0.2 mm, n = 120 RPM) matched with that

of the experiments, which validated the effectiveness of calculation method proposed.

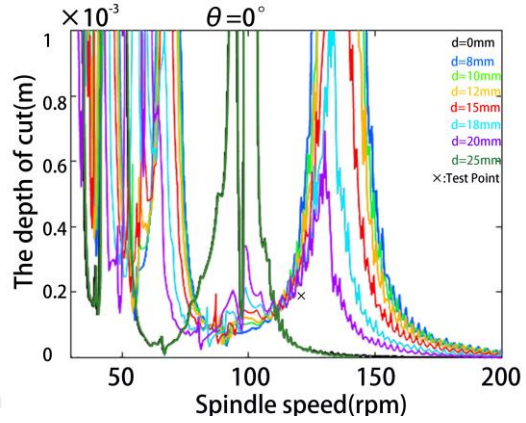

Figure 7. Stability lobes of boring bars with holes of different diameters.

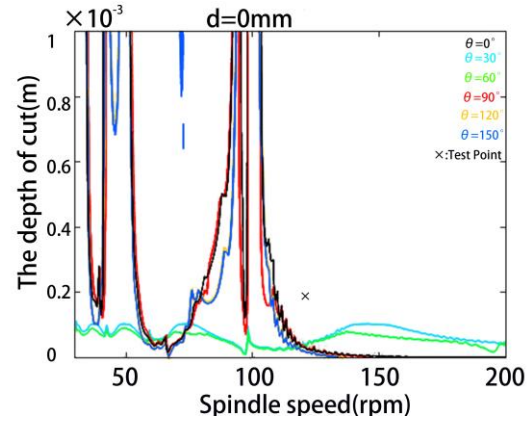

Figure 8. Stability lobes of boring bars without holes at different θ.

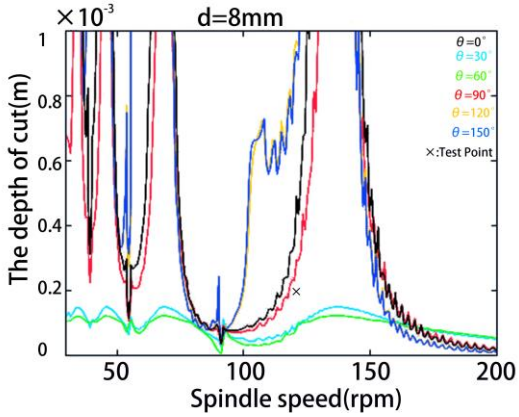

Figure 9. Stability lobes of boring bars with 8 mm diameter holes at different θ.

From Fig. 7, the stability lobes calculated by this method showed that when θ was 0 and d was 0 or 25 mm, the test point X (under the operating condition of the experiments) was in an unstable area. When d was 8, 10, 12, 15, 18, or 20 mm, the test point X was in a stable area. Furthermore, when d was 8 mm, the test point X was farthest from the dividing line.

From Fig. 8, the stability lobes calculated by this method showed that when d was 0 and θ was 0°, 30°, 60°, 90°, 120°, or 150°, the test point X was in an unstable area. Furthermore, when θ was 150°, the test point X was farthest from the dividing line.

From Fig. 9, the stability lobes calculated by this method showed that when d was 8 mm and θ was 30° or 60°, the test point X was in an unstable area, but when θ was 0°, 90°, 120°, or 150°, the test point X was in a stable area. Furthermore, when θ was 150°, the test point X was farthest from the dividing line.

Comparing Fig. 8 with Fig. 9, when θ was constant, it is evident that adding holes in the boring bar can decrease the chatter.

Similar experimental results were shown in [18], from which it could be seen that, first, when d of the boring bar was 0, the vibration speed was greater than that of a boring bar with holes, regardless of the θ; second, when θ was 0° and d was 0 or 25 mm, the vibration speed was greater than that of other sized holes; third, when d was not 0, the vibration speed decreased. The influence of each parameter on the amplitude of the boring chatter was consistent with those of the stability lobes.

V. Conclusion

A model of the 3-DOF boring process was established. Using boring force and boring thickness modeling, the relationship between the boring forces and the displacements in three directions of the 3-DOF boring kinematics equations were deduced. Stability analysis of the kinematics equation was solved using the second-order full-discretization method.

Using the calculation method proposed in this work, the stabilities of boring bars with different parameters were analyzed. The results matched with those of experiments, which validated the effectiveness of the proposed method. The calculated stability lobes can therefore be used to optimize the design parameters of boring bars.

Acknowledgment

This research was financially supported by the National Nature Science Foundation of China (Grant No. 51575301), and Shenzhen Foundational Research Project (Grant No. JCYJ20160428181916222).

References

[1] G. Quintana, and J. Ciurana. “Chatter in machining processes: A review”. In: *International Journal of Machine Tools & Manufacture*, 51.5,2011, pp.363-376.

[2] J. Tlusty, and L. Spacek. *Self-excited vibration in machine tools*. Prague, 1954.

[3] T. R.Sisson, and R. L. Kegg. “An Explanation of Low-Speed Chatter Effects”. In: *Journal of Manufacturing Science & Engineering* 91.4,1969.

[4] A.Gasparetto. “Eigenvalue Analysis of Mode-Coupling Chatter for Machine-Tool Stabilization” .In: *Journal of Vibration & Control*, 7.2, 2001, pp: 181-197.

[5] A. Iturrospe, V. Atxa, and J. M.Abete “State-space analysis of mode-coupling in orthogonal metal cutting under wave regeneration”.

In: *International Journal of Machine Tools & Manufacture*, 47.10, 2007, pp. 1583-1592.

[6] J. Tlusty, and F. Ismail. “Basic Non-Linearity in Machining Chatter”. In: *CIRP Annals - Manufacturing Technology*, 30.1, 1981, pp.299-304.

[7] E. Budak, and Y. Altintas. “Analytical Prediction of Chatter Stability in Milling—Part I:General Formulation”. In: *Journal of Dynamic Systems Measurement & Control*, 120.1, 1998, pp.31-36.

[8] Y. Altintaş, and E. Budak. “Analytical Prediction of Stability Lobes in Milling”. In: *CIRP Annals - Manufacturing Technology*, 44.1,1995, pp.357-362.

[9] S. D. Merdol, and Y. Altintas. “Multi Frequency Solution of Chatter Stability for Low Immersion Milling”. In: *Journal of Manufacturing Science & Engineering*, 126.3, 2004, pp.459-466.

[10] T. Insperger, and G. Stepan. “Semi‐discretization method for delayed systems”. In: *International Journal for Numerical Methods in Engineering*, 55.5, 2010, pp.503-518.

[11] Y. Ding, L.M. Zhu, X.J. Zhang, and H. Ding. “A full-discretization method for prediction of milling stability”. In: *International Journal of Machine Tools & Manufacture*, 50.5, 2010, pp.502-509.

[12] P. V. Bayly, J. E. Halley, B. P. Mann, and M. A. Davies. “Stability of Interrupted Cutting by Temporal Finite Element Analysis”. In: *Journal of Manufacturing Science & Engineering*, 125.2, 2003, pp.220-225.

[13] J. Tlusty, and F. Ismail. “Special Aspects of Chatter in Milling”. In: *Journal of Vibration & Acoustics*, 105.1, 1983, pp.24.

[14] S. Smith, J. Tlusty. “Efficient Simulation Programs for Chatter in Milling”. In: *CIRP Annals - Manufacturing Technology*, 2.1,1993, pp.4463-466.

[15] C. Xu, J.F. Zhang, P.F. Feng, D.W. Yu, and Z.J. Wu. “Characteristics of stiffness and contact stress distribution of a spindle-holder taper joint under clamping and centrifugal forces”. In: *International Journal of Machine Tools & Manufacture*. 82-83.7, 2014, pp.21-28.

[16] J.P Liao, D.W. Yu, J.F. Zhang, P.F. Feng, and Z.J. Wu. “An efficient experimental approach to identify tool point FRF by improved receptance coupling technique”. In: *The International Journal of Advanced Manufacturing Technology.* January 2018, Volume 94, Issue 1–4, pp. 1451–1460.

[17] Y. Ding, L.M. Zhu, X.J. Zhang, and H. Ding. “Second-order full-discretization method for milling stability prediction”. In: *International Journal of Machine Tools and Manufacture*, 50.10, 2010, pp. 926-932.

[18] L.N. Xu. “Research on oscillation mode coupling of boring bar”. M.S. thesis, Dept. Mecha. Eng. Zhengzhou Univ, Zhengzhou, China, 2009.